Dissolution of Eucalyptus Powder with Alkaline Ionic Liquid [Mmim]DMP under Microwave Conditions

Tiantian Chen,[a,b] Youming Li,[a,b] Junxin Xu,[a,b] and Yi Hou [a,b,]*

An orthogonal design was used to study three factors—melting temperature, time, and solid-liquid ratio—and how they affected the dissolution rate of eucalyptus powder. The optimum solution conditions were 170 °C, 20 min, and a solid-liquid ratio of 1:25. Composition analysis of the residue indicated that, in the dissolving process, acid-insoluble lignin was converted into acid-soluble lignin, and a part of the lignin was degraded or modified. After dissolution, the crystalline structure of cellulose deteriorated, the relative crystallinity decreased, and the crystal form changed from type I into amorphous. Wood powder degradation occurred during dissolution, and a higher dissolution rate led to greater degradation. In a low-temperature environment below 225 °C, the residue thermal stability decreased slightly with increasing dissolution rates, but it greatly improved in a high-temperature environment of 225 to 600 °C.

Keywords: Ionic liquid; Microwave; Solubility; Lignin; Lignocellulose

Contact information: a: State Key Laboratory of Pulp and Paper Engineering, South China University of Technology, Guangzhou 510640, China; b: National Engineering Research Center of Papermaking and Pollution Control, South China University of Technology, Guangzhou 510640, China;
** Corresponding author: ceyhou@scut.edu.cn*

INTRODUCTION

Lignocellulose is the most abundant renewable resource on the planet. Its main components of cellulose, hemicellulose, and lignin are important chemical raw materials (Zhang 2008; King *et al.* 2009; Kuo and Lee 2009; Zhang *et al.* 2009). However, due to the complex structure of lignocellulosic cell wall, its components are difficult to separate, which is a great obstacle in using lignocellulose (Chen and Kuo 2010). Traditional separation methods are cooking with inorganic acid or alkali and extraction with organic solvents. These methods not only change lignocellulosic structure but also have the problems of high cost and serious pollution. Ionic liquids are green solvents with low vapor pressure, adjustable nature, good solubility, and high thermal stability (Rehman and Zeng 2012; Lozano *et al.* 2014; Findrik *et al.* 2016), and they have broad application prospects in the dissolution and separation of lignocellulose (Cole *et al.* 2002; Fang *et al.* 2006; Ren *et al.* 2013).

Previous literature includes studies of the dissolution of a single component with ionic liquids. Some alkyl-substituted imidazolium ionic liquids effectively dissolve cellulose (Swatloski *et al.* 2002). An ionic liquid solvent [C_4mim]Cl dissolves hemicellulose (Ren *et al.* 2007). The ionic liquids [Mmim][CH_3SO_4] and [C_4mim][CH_3SO_4] dissolve lignin at room temperature (Pu *et al.* 2007). However, because of the complicated structure of lignocellulose, the dissolution rate of whole components with ionic liquids is not high. In a study on the dissolution of Masson pine, poplar, eucalyptus, and oak in the [C4mim]Cl/DMSO solvent system, non-pretreated lignocellulose heated to 100 °C for 24 h could be partially dissolved (Fort *et al.* 2007). The low dissolution rate of all components is an urgent problem hindering the use of biomass resources.

To promote the application of ionic liquids in biomass materials and improve the dissolution rate of whole components, the present work involves an orthogonal design for the lignocellulosic dissolution factors of melting temperature, time, and solid-liquid ratio under microwave conditions, and the optimized solution scheme was determined. The chemical composition of the residue was analyzed to find variations in the three components during dissolution. Four types of residue with different dissolution rates were selected to study structural changes.

EXPERIMENTAL

Synthesis of Ionic Liquid [Mmim]DMP

Trimethyl phosphate was added to N-methyl imidazole at a 1.2:1 ratio in a nitrogen atmosphere. The system was heated to 110 °C and reacted for 10 h. The obtained product was washed three times with diethyl ether, with vacuum distillation for 6 h and vacuum drying at 60 °C for 6 h. The resulting [Mmim]DMP was a light yellow and transparent liquid (Fig. 1; Nie *et al.* 2006; Li *et al.* 2009). The yield and purity were 97.98% and 99.77%, respectively.

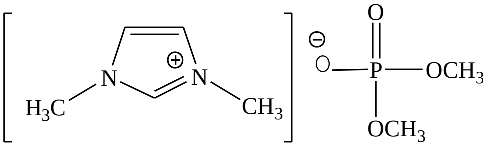

Fig. 1. Structure of ionic liquid [Mmim]DMP

Determination of [Mmim]DMP Yield

Yield was determined using the following equation,

$$Y = A/B * 100\ \% \tag{1}$$

where Y is yield of Ionic liquid [Mmim]DMP and A is the actual quantity of ionic liquid. The symbol B represents the theoretical quantity of ionic liquid.

Determination of [Mmim]DMP Purity

Purity was determined by utilizing ultraviolet spectrophotometry, following the procedure described by Łuczak (Łuczak *et al.* 2008)

Determination of Viscosity

Viscosity of the samples after centrifuging were determined at 25 °C using the rotator viscometer (RVDV-II+PRO, USA).

Analytical Methods

Wood powder in the particle size in the range of 40 to 60 mesh, after benzene alcohol extraction, was poured into ionic liquid and dissolved in a microwave environment (XH-100B, Xianghu Company, Beijing, China) with heating power of 500 W. When the system was cooled down, it was centrifuged to separate solid and liquid phases. The residue was washed with distilled water, and the dissolution rate was calculated from the weight of residue. Scanning electron microscopy (SEM; EV018, Carl Zeiss AG, Oberkochen, Germany) was used to observe the surface micro-structure of residue in a vacuum. The solid-liquid (solid-liquid ratio of 1:25) reaction system was observed by perpendicular polarizing microscopy (PLM; DM2700M, Leica Microsystems GmbH, Wetzlar, Germany). Infrared spectra of samples were measured by a Fourier transform infrared spectrometer (Vector 33, Bruker, Karlsruhe, Germany). X-ray diffraction (XRD) was carried out using a diffraction instrument (Bruker D8 ADVANCE). Thermogravimetric analysis was completed by a TAQ500 instrument (TA Company, New Castle, USA) in a nitrogen atmosphere, and a heating rate of 15 °C/min from 25 to 600 °C. The UV spectra were obtained on a Scinco S-3100 UV spectrophotometer (Hach, Loveland, CO, USA). The nuclear magnetic resonance (NMR) were measured on the Superconducting Fourier Transform Nuclear Magnetic Resonance Spectrome (Bruker, Germany). The chemical composition analysis methods are shown in Table 1.

Table 1. Methods Used to Determine the Chemical Composition of Eucalyptus

Chemical Composition Test	Standard
Pentosans in wood	GB/T 2677.9 (1994)
Holocellulose in wood	GB/T 2677.10 (1995)
Acid-soluble lignin in wood	GB/T 10337 (1989)
Acid-insoluble lignin in wood	GB/T 2677.8 (1994)

RESULTS AND DISCUSSION

Infrared (IR) spectra and nuclear magnetic resonance (NMR) analysis

Infrared (IR) spectra of the standard [Mmim]DMP and laboratory-synthesized sample are shown in Fig. 2. The two curves are quite similar. The peaks of 3110 and 3157.3 cm^{-1} are C-H stretching vibration absorptions; 1575.8 cm^{-1} is the C=N stretching vibration peak; 1236.3 cm^{-1} is the P=O stretching vibration absorption; 1178.5 cm^{-1} shows C-H in-plane flexural vibration. The peak of 1045.4 cm^{-1} is the P-OR stretching vibration absorption. It can be assumed that laboratory-synthesized sample can be considered as [Mmim]DMP.

^{1}H-NMR spectra of the standard [Mmim]DMP and laboratory-synthesized sample are shown in Fig. 3. The chemical shift of methyl H on the imidazole ring is 3.469 ppm; 3.782 ppm is the chemical shift of methyl H in dimethyl phosphate. The chemical shift of methyl H connecting N+ on the imidazole ring is 4.701 ppm. The chemical shift of hydrogen atom of HC=CH on the imidazole ring is 7.302 ppm; 8.538 ppm is the chemical shift of hydrogen atom of –CH= connecting nitrogen on the imidazole ring. Due to residual trimethyl phosphate, the peak of H-2 is the strongest in the ^{1}H-NMR spectra and H-3 is behind it, which is adverse to the laboratory-synthesized sample.

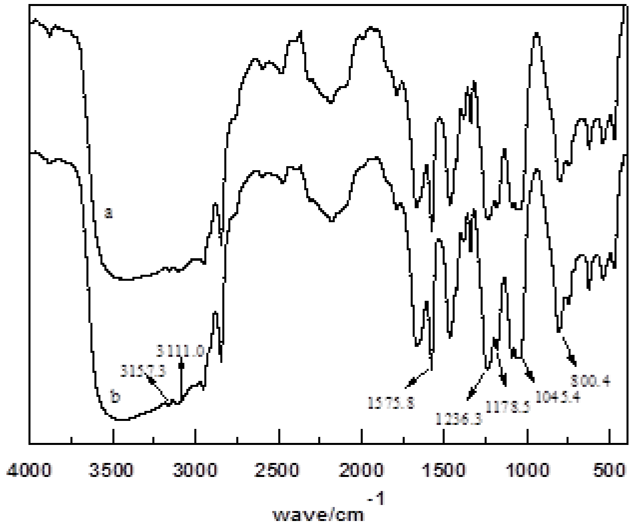

Fig. 2. FT-IR spectra of [Mmim]DMP. (a) standard [Mmim]DMP (b) laboratory-synthesized sample

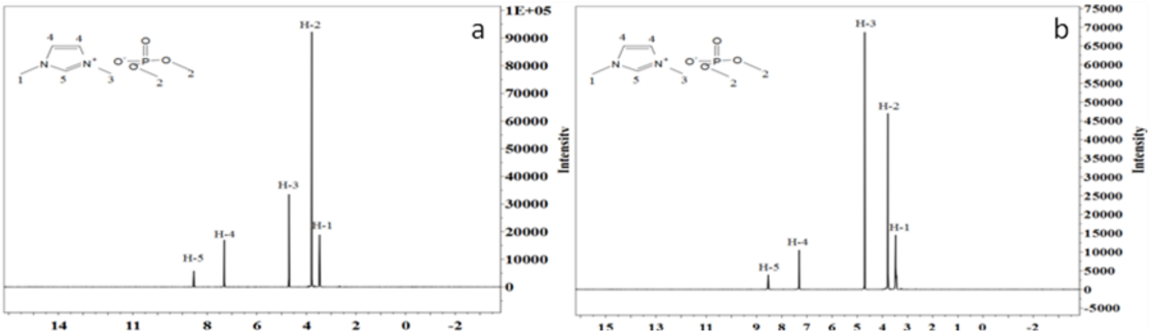

Fig. 3. ^{1}H-NMR spectra of [Mmim]DMP. (a) standard sample (b) laboratory-synthesized sample

^{13}C-NMR spectra of the standard [Mmim]DMP and laboratory-synthesized sample are shown in Fig. 4. The chemical shift of carbon atom of –CH= connecting nitrogen is 8.538 ppm. The chemical shift of carbon atom of HC=CH on the imidazole ring is 7.302 ppm. The chemical shift of methyl C in dimethyl phosphate is 3.469 ppm, and 35.552 ppm is the chemical shift methyl C connecting –NH-. The peak intensity of the standard sample and laboratory-synthesized sample is basically the same. So the laboratory-synthesized sample is considered to be [Mmim]DMP.

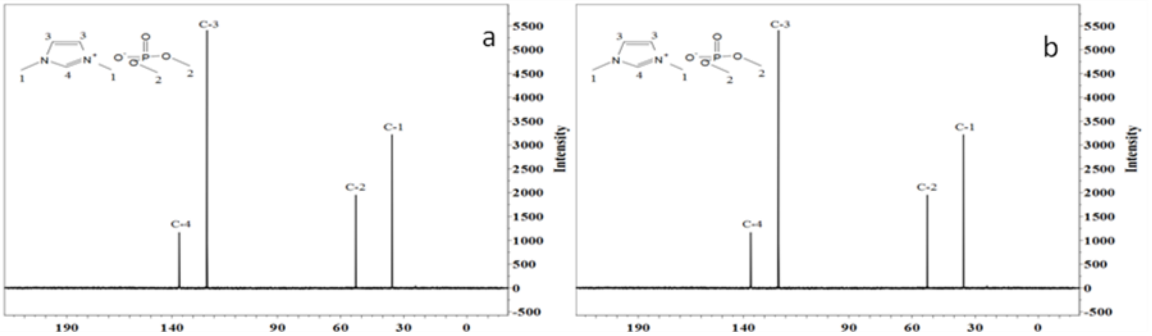

Fig. 4. ^{13}C-NMR spectra of [Mmim]DMP. (a) standard sample (b) laboratory-synthesized sample

Influence of Reaction Environment on Solubility of Whole Components

The selected dissolution condition was a solid-liquid ratio (weight solid by weight solution) of 1:30 and melting temperature of 170 °C. Wood powder solubility in microwave and normal environment is shown in Table 2. The dissolution rate in the microwave environment was up to 88.39% higher than in a room environment at the same reaction time of 20 min. Microwaving for 20 min was nearly 50% better than the reaction in the common environment for 30 h. The microwave reaction greatly improved dissolution rates. Because its efficiency was much greater than conventional reaction, it created a possibility for component separation and utilization of biomass resources.

Table 2. Wood Powder Solubility in Different Reaction Environments

Reaction environment	20 min in microwave environment	20 min in room environment	30 h in room environment
Solubility of wood powder (%)	95.06	6.67	45.84

Microwave Dissolution of Wood Powder by Orthogonal Design

Dissolution of wood powder involves many factors. By single factor experiment analysis, three factors that greatly influence the dissolution rates of wood powder were determined: melting temperature, time, and solid-liquid ratio. An orthogonal design was used to study the impact of these factors on the dissolution rates, significantly reducing the number of experiments to optimize target parameters. Three levels of each factor were selected, and an L9 (3^4) orthogonal table was used to design experiments (Table 3).

Table 3. Factors and Levels in Microwave Dissolution of Wood Powder

Level	A. Melting Temperature (°C)	B. Time (min)	C. Solid-Liquid Ratio
1	160	15	1:25
2	170	20	1:30
3	180	25	1:35

The impacts of the three factors on wood powder solubility are listed as follows, in order of importance: melting temperature > time > solid-liquid ratio (Table 3). The upper and lower limits were chosen for each factor according to previous studies. $A_3B_2C_1$ was the best combination scheme (test no. 8), but the dissolution rate in these conditions was slightly less than $A_2B_2C_3$ (test no. 5). The solid-liquid ratio had little impact on solubility, so the combination scheme $A_2B_2C_1$ was selected after considering the energy consumption and cost.

With the amount of solvent, increasing the amount of solute would increase the density and so the viscosity would become larger. This combination included a melting temperature of 170 °C, time of 20 min, and solid-liquid ratio of 1:25. As confirmed by experimental results, the solubility was 94.91%, which was close to the maximum of the orthogonal experiment; thus, the optimized process was stable. There was a positive correlation between sample viscosity and dissolution rates. A higher dissolution rate resulted in greater viscosity.

Table 4. Orthogonal Test Results and Analysis of Wood Powder Dissolution

Test Number	Factors				Solubility (%)	Viscosity (cP) *
	A. Melting Temperature (°C)	B. Time (min)	C. Solid-Liquid Ratio	D. Blank		
1	160	15	1:25	1	13.26	153
2	160	20	1:30	2	17.53	202
3	160	25	1:35	3	18.82	218
4	170	15	1:30	3	31.84	369
5	170	20	1:35	1	97.82	1134
6	170	25	1:25	2	95.12	1103
7	180	15	1:35	2	45.76	530
8	180	20	1:25	3	95.89	1112
9	180	25	1:30	1	96.34	1117
K_1	16.54	30.29	68.09	69.14		
K_2	74.93	70.41	48.57	52.80		
K_3	79.33	70.09	54.13	48.85		
R	62.79	40.12	19.52	20.29		
* Viscosity was measured at 25 °C						

Residue's Chemical Composition with Different Temperatures

Selected dissolving conditions were a time of 5 min, solid-liquid ratio of 1:30, and melting temperatures of 140, 150, 160, 170, and 180 °C. The hemicellulose and lignin contents (holocellulose, pentosane) of the obtained residue are shown in Table 5.

Table 5. Residue Chemical Composition with Different Temperatures

Temperature (°C)	140	150	160	170	180
Solubility (%)	2.76	5.38	8.91	14.22	14.64
Holocellulose (%)	77.79	75.73	76.17	63.67	64.00
Pentosan (%)	26.04	24.44	23.54	20.94	19.44
Lignin (%)	18.56	17.69	19.20	21.11	20.00
Acid-insoluble Lignin (%)	12.41	10.91	11.01	9.45	8.71
Acid-soluble Lignin (%)	6.15	6.79	8.19	11.66	11.29

Table 6. Chemical Composition of Eucalyptus

Chemical Components	Holocellulose	Lignin		Pentosan
		Acid-insoluble	Acid-soluble	
Content (%)	75.19	27.32	2.75	25.44
		30.07		

According to Tables 5 and 6, as the temperatures rose, the residue content of holocellulose and pentosan decreased, while the lignin content rose. At the beginning of the solution, ionic liquid of lignin solution were in the dominant position, and with the increase in the dissolution rate, the degree of dissolution of cellulose and hemicellulose increased, so the content of lignin content in the residue increased. Compared with raw material, the holocellulosic content of residue at the temperatures of 140 to 160 °C was improved and reached a maximum at 140 °C increasing by 2.60%. It decreased between 160 and 180 °C especially at the sharpest decline between 160 and 170 °C. The pentosan content increased at 140 °C and then sharply declined between 160 and 170 °C.

Compared with raw material, the lignin content obviously declined and reached a minimum at 150 °C, decreasing by 12.38%. The amount of decline accounted for 41.17% of the original lignin. In addition, the acid-insoluble lignin content obviously decreased and reached a minimum at 180 °C falling by 18.61% compared with raw material. The amount of decline accounted for 68.12% of the original acid-insoluble lignin. Acid-soluble lignin content had a substantial increase and reached a maximum at 170 °C, rising by 8.91%.

During microwave treatment, ionic liquid dissolved eucalyptus lignin, improving its molecular accessibility. Acid-insoluble lignin was converted to acid-soluble lignin, with partial lignin degradation or modification.

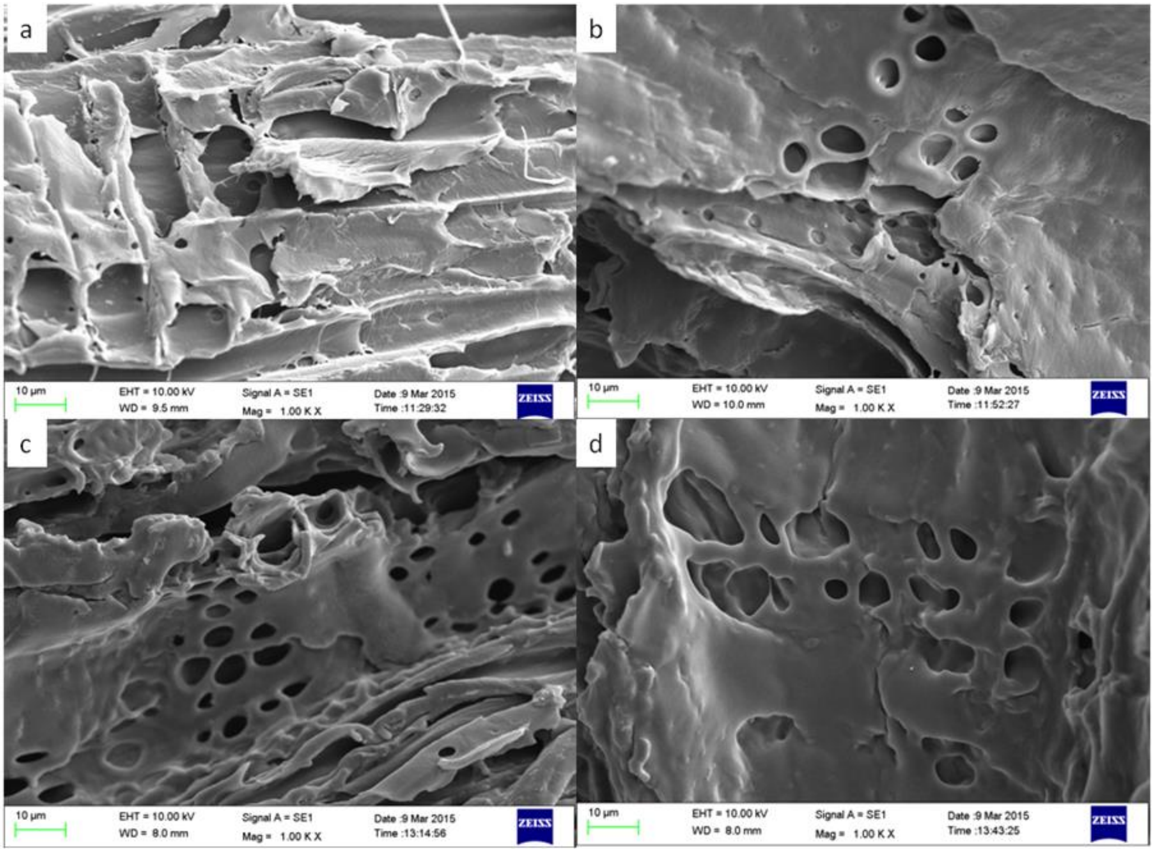

Fig. 5. SEM images of residue at 1000x magnification. (a) 8.91% solubility, (b) 18.82% solubility, (c) 31.84% solubility, and (d) 45.76% solubility

SEM Observation of Eucalyptus Residue Structure

Because wood powder was almost all dissolved under the high dissolution rate, there was very little residue available for SEM observation. To better analyze the dissolution process, four types of residue with low solubility were selected for SEM. Residue with solubility of 8.91% had a fluffy structure and numerous ravines with external fibrillation. Residue with solubility of 18.82% had a poroid structure with a sheet overlap, and ravines disappeared. The poroid structure became more apparent and depressed with solubility of 31.84%, making a deteriorated surface regularity. When the solubility was 45.76%, the residue structure formed a shape of karst landform having an obvious erosive and dissolved trace, and the interlayer structure was no longer apparent. Thus, the ionic liquid [Mmim]DMP dissolved eucalyptus powder by infiltrating layer upon layer from the outer to the inner to gradually destroy lignocellulosic overall structure.

PLM Observation of Wood Powder Microwave Dissolving Process

Under the preferred dissolution condition (170 °C, 20 min, a solid-liquid ratio of 1:25), PLM images of the solid-liquid heterogeneous reaction system were captured at different time points. The lignocellulose had an elongated rod shape, and the white area in images was the crystalline region of cellulose. During dissolution, the crystal was gradually eliminated. When the reaction proceeded to 12 min, lignocellulosic particles began to disperse uniformly in the ionic liquid and exhibited a highly bright micro morphology with irregular flakes, indicating that a part of lignocellulosic particles had not been infiltrated by ionic liquid. When the dissolved time was 20 min, the mixture was a single-phase homogeneous system. The solution was almost uniformly euphotic and isotropic, which illustrated that lignocellulosic particles were almost completely dissolved in the ionic liquid.

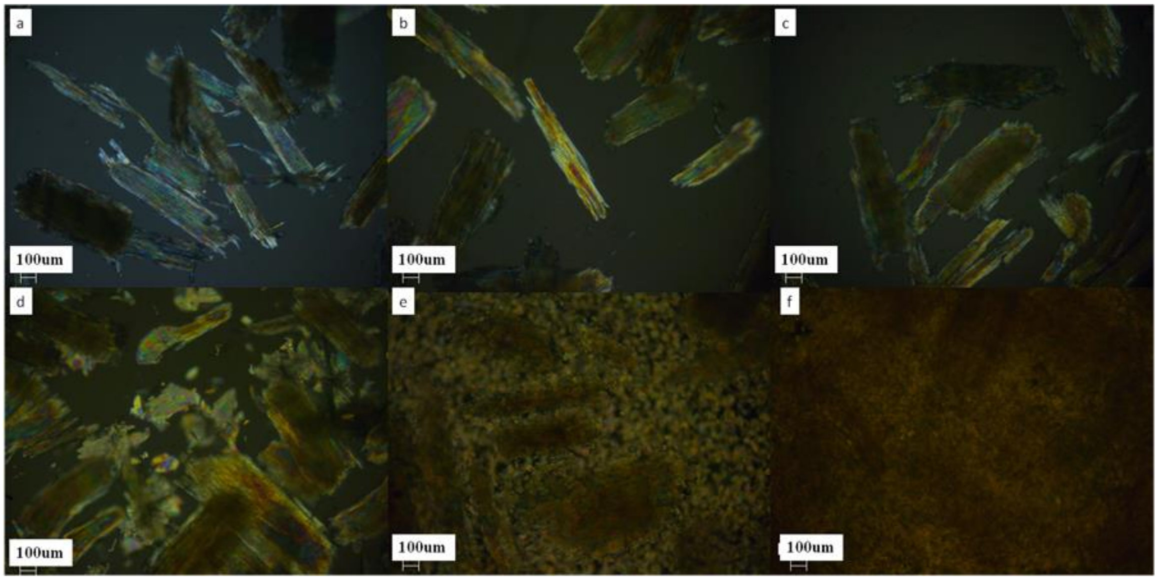

Fig. 6. Influence of dissolved time on the lignocellulosic dissolution. (a) Untreated, (b) 4 min, (c) 8 min, (d) 12 min, (e) 16 min, and (f) 20 min under 250x magnification

Eucalyptus Residue XRD Analysis after Microwave Dissolution

Figure 7 shows that after microwave dissolution, eucalyptus residue with solubilities of 8.91% and 18.82% had typical and characteristic diffraction peaks of cellulosic type I that appeared at 2θ angles of 16° and 22°. With increased solubility, the peak intensity at 16° was weakened. When solubility was more than 31.84%, the characteristic peak near 16° disappeared, but the characteristic peak that is diffraction patterns characteristic of amorphous cellulose at 22° was present. The characteristic peak's position was shifted to a lower 2θ value. Peak value decreased, and its shape was broadened with increased solubility. After dissolution, the cellulosic crystalline regularity became worse as solubility increased. The relative crystalline degree was reduced, and the crystal form changed from type I to amorphous.

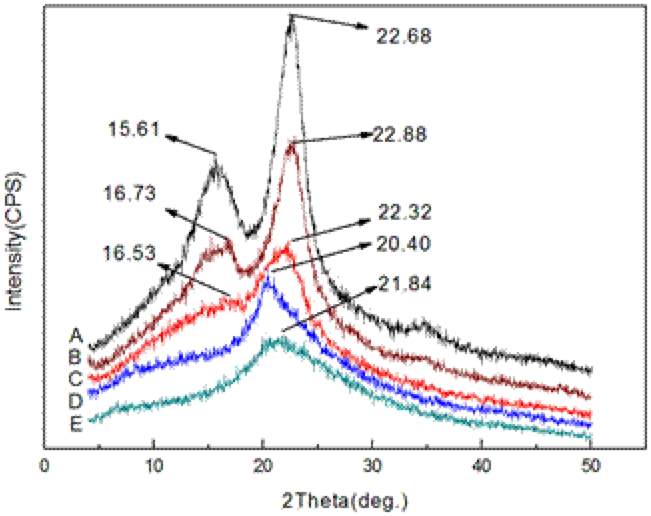

Fig. 7. XRD spectra of eucalyptus residue with different solubilities. (A) raw material, (B) 8.91% solubility, (C) 18.82% solubility, (D) 31.84% solubility, and (E) 45.76% solubility

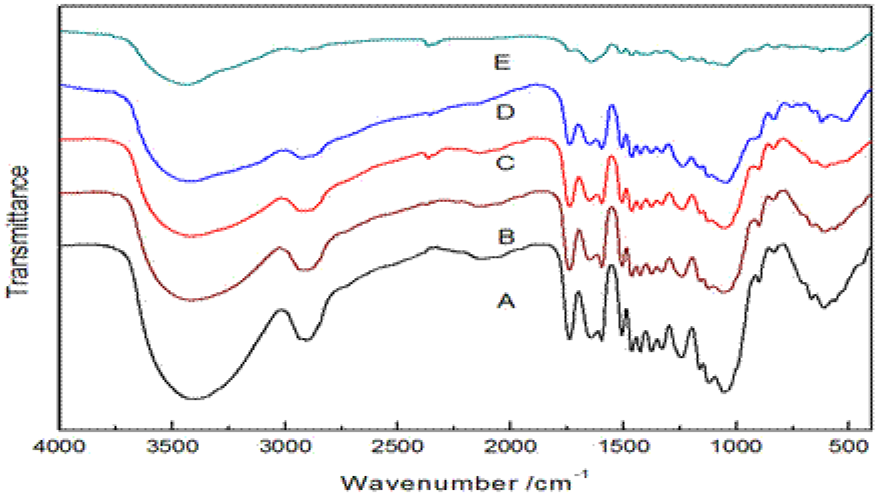

Fig. 8. Infrared spectra of eucalyptus residue with different solubilities. (A) raw material, (B) 8.91% solubility, (C) 18.82% solubility, (D) 31.84% solubility, (E) 45.76% solubility

Electron donor-acceptor (EDA) theory could explain this phenomenon. N-methyl imidazolium cation and dimethyl phosphate anion of the ionic liquid [Mmim]DMP, respectively, as electron acceptor and electron donor centers, interacted with H and O atoms of cellulosic -OH to produce EDA complexes (Pinkert *et al.* 2010; Gupta and Jiang 2015; Zhang *et al.* 2015). They led to hydrogen bond fracture between cellulosic macromolecules, which deteriorated crystalline regularity. Because of ionic liquid's strong polarity, cellulosic intramolecular hydrogen bonding was weakened. The molecular chains were open to varying degrees, so that cellulose was partially dissolved. With a higher open degree of molecular chains, accessibility of lignin and cellulosic molecules was improved, and solubility was greater as well.

Infrared Spectra Analysis after Microwave Dissolution

In the infrared spectrum of Fig. 8, the raw material peak shapes were sharp, and crests had large intensities. With increased solubility, peak shapes became blunt and wide until they disappeared, and peak intensities decreased. When solubility was 45.76%, the peak was barely visible, indicating that the three chemical constituents were dissolved, and molecular accessibility was improved. Each characteristic functional group was destroyed, and the extent of damage increased further when the solubility increased. Wood powder degradation occurred during dissolution, and the degree of degradation was greater with a higher dissolution rate.

Eucalyptus Residue's TG Analysis after Microwave Dissolution

As shown in Fig. 9, thermal weight losses of eucalyptus raw material and residue were divided into three phases. In phase I, material weights were constant without decomposition. Phase II was the stage of raw material thermal decomposition with a fast speed. Phase III was included the decomposition of remaining coking substances and formation of ash; the thermal decomposition rates and weight loss rates were small.

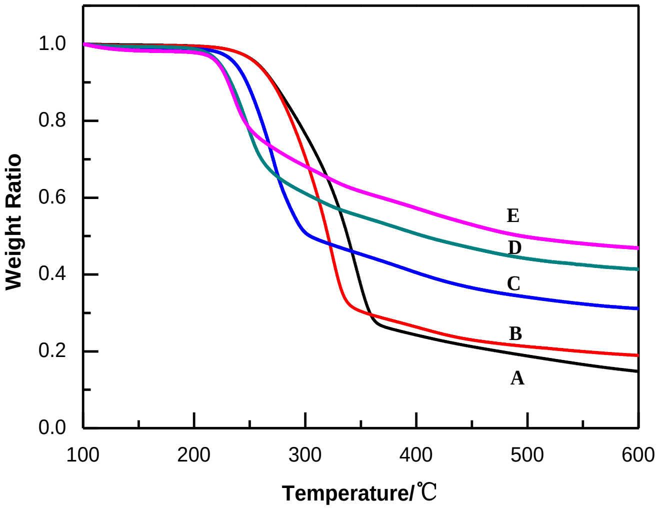

Fig. 9. TG curves of *eucalyptus* residue with different solubilities. (A) raw material, (B) 8.91% solubility, (C) 18.82% solubility, (D) 31.84% solubility, (E) 45.76% solubility

Table 7. Eucalyptus Residue TG Analysis

Solubility (%)	TG Phase I		TG Phase II		TG Phase III	
	Temp (°C)	Weight Loss (%)	Temp (°C)	Weight Loss (%)	Temp (°C)	Weight Loss (%)
0	100-224.2	1.07	224.2-363.5	72.37	363.5-600	85.25
10.02	100-223.4	1.06	223.4-338.7	67.49	338.7-600	81.07
18.82	100-217.0	1.82	217.0-301.0	49.30	301.0-600	68.90
31.84	100-210.8	2.13	210.8-261.4	30.40	261.4-600	58.51
45.76	100-208.0	2.63	208.0-244.9	19.87	244.9-600	53.12

Table 7 indicates that with increased solubility, the initial thermal decomposition temperatures of residue decreased, and the weight loss rates increased in phase I. These changes were attributed to decreasing crystallinity. This result indicated that in the low-temperature environment below 225 °C, the residue thermal stability was weakened slightly with the solubility increase. Final temperatures of phase II also showed a decreasing trend with increasing solubility, and weight losses were obviously reduced, indicating that thermal decomposition of organic matters including carbohydrate and lignin in residue was easier. Weight losses of phase III decreased sharply with improved solubility, illustrating that the thermal stability of residue was greatly improved between 225 and 600 °C. Therefore, in the process of dissolution, the three components continued dissolution greatly increased inorganic content in the residue, such as ash, and organic content was drastically reduced.

CONCLUSIONS

1. Microwave treatment promoted the dissolution of all biomass components, increasing the solubility from 6.67% to 95.06%. The orthogonal design in microwave dissolution showed that the factors affecting wood powder solubility were, in order of importance, melting temperature, time, and solid-liquid ratio. The optimum dissolving condition was 170 °C, 20 min, and a solid-liquid ratio of 1:25. Under this condition, the solubility was 94.91%.
2. During microwave dissolving, ionic liquid dissolved eucalyptus lignin, improving lignin molecular accessibility. Acid-insoluble lignin was converted to acid-soluble lignin, with partial lignin degradation or modification.
3. The ionic liquid [Mmim]DMP dissolved eucalyptus powder by infiltrating layer upon layer from the outer to the inner, to gradually destroying lignocellulosic overall structure. After dissolution, the cellulosic crystalline regularity became with increased solubility. The relative crystalline degree was reduced, and crystal form changed from type I into amorphous. Wood powder degradation occurred during dissolution, and the degree of degradation was greater with a higher dissolution rate. In addition, the three components continued to dissolve into inorganic content in residue, and organic content was drastically reduced.

ACKNOWLEDGMENTS

This research was supported by State Key Laboratory of Pulp and Paper Engineering Foundation (2015C02), Science and Technology Planning Project of Guangdong Province (2015A020215009), and the National Natural Science Foundation of China (21206046, 21476091).

REFERENCES CITED

Chen, W., and Kuo, P. (2010). "A study on torrefaction of various biomass materials and its impact on lignocellulosic structure simulated by a thermogravimetry," *Energy* 35(6), 2580-2586. DOI: 10.1016/j.energy.2010.02.054

Cole, A. C., Jensen, J. L., Ntai, I., Tran, K. L. T., Weaver, K. J., Forbes, D. C., and Davis, J. H. (2002). "Novel Brønsted acidic ionic liquids and their use as dual solvent-catalysts," *Journal of the American Chemical Society* 124(21), 5962-5963. DOI:

10.1021/ja026290w

Fang, D., Zhou, X., Ye, Z., and Liu, Z. (2006). "Brønsted acidic ionic liquids and their use as dual solvent-catalysts for Fischer esterifications," *Industrial & Engineering Chemistry Research* 45(24), 7982-7984. DOI: 10.1021/ie060365d

Findrik, Z., Megyeri, G., Gubicza, L., Bélafi-Bakó, K., Nemestóthy, N., and Sudar, M. (2016). "Lipase catalyzed synthesis of glucose palmitate in ionic liquid," *Journal of Cleaner Production* 112, 1106-1111. DOI: 10.1016/j.jclepro.2015.07.098

Fort, D. A., Remsing, R. C., Swatloski, R. P., Moyna, P., Moyna, G., and Rogers, R. D. (2007). "Can ionic liquids dissolve wood? Processing and analysis of lignocellulosic materials with 1-n-butyl-3-methylimidazolium chloride," *Green Chem.* 9(1), 63-69. DOI: 10.1039/B607614A

Gupta, K. M., and Jiang, J. (2015). "Cellulose dissolution and regeneration in ionic liquids: A computational perspective," *Chemical Engineering Science* 121, 180-189. DOI: 10.1016/j.ces.2014.07.025

King, A. W. T., Zoia, L., Filpponen, I., Olszewska, A., Xie, H., Kilpeläinen, I., and Argyropoulos, D. S. (2009). "*In situ* determination of lignin phenolics and wood solubility in imidazolium chlorides using ^{31}P NMR," *Journal of Agricultural and Food Chemistry* 57(18), 8236-8243. DOI: 10.1021/jf901095w

Kuo, C., and Lee, C. (2009). "Enhanced enzymatic hydrolysis of sugarcane bagasse by N-methylmorpholine-N-oxide pretreatment," *BioResource Technology* 100(2), 866-871. DOI: 10.1016/j.biortech.2008.07.001

Li, Q., He, Y. C., Xian, M., Jun, G., Xu, X., Yang, J. M., and Li, L. Z. (2009). "Improving enzymatic hydrolysis of wheat straw using ionic liquid 1-ethyl-3-methyl imidazolium diethyl phosphate pretreatment," *BioResource Technology* 100(14), 3570-3575. DOI: 10.1016/j.biortech.2009.02.040

Lozano, P., Bernal, B., Jara, A. G., and Belleville, M. (2014). "Enzymatic membrane reactor for full saccharification of ionic liquid-pretreated microcrystalline cellulose," *BioResource Technology* 151, 159-165. DOI: 10.1016/j.biortech.2013.10.067

Łuczak, J., Hupka, J., Thöming, J., and Jungnickel, C. (2008). "Self-organization of imidazolium ionic liquids in aqueous solution," *Colloids & Surfaces A Physicochemical & Engineering Aspects* 329(3), 125-133. DOI: 10.1016/j.colsurfa.2008.07.012

Nie, Y., Li, C., Sun, A., Meng, H., and Wang, Z. (2006). "Extractive desulfurization of gasoline using imidazolium-based phosphoric ionic liquids," *Energy & Fuels* 20(5), 2083-2087. DOI: 10.1021/ef060170i

Pinkert, A., Marsh, K. N., and Pang, S. (2010). "Reflections on the solubility of cellulose," *Industrial & Engineering Chemistry Research* 49(22), 11121-11130. DOI: 10.1021/ie1006596

Pu, Y., Jiang, N., and Ragauskas, A. J. (2007). "Ionic liquid as a green solvent for lignin," *Journal of Wood Chemistry and Technology* 27, 23-33. DOI: 10.1080/02773810701282330

Rehman, A., and Zeng, X. (2012). "Ionic liquids as green solvents and electrolytes for robust chemical sensor development," *Accounts of Chemical Research* 45(10), 1667-1677. DOI: 10.1021/ar200330v

Ren, H., Zhou, Y., and Liu, L. (2013). "Selective conversion of cellulose to levulinic acid *via* microwave-assisted synthesis in ionic liquids," *BioResource Technology* 129, 616-619. DOI: 10.1016/j.biortech.2012.12.132

Ren, J. L., Sun, R. C., Liu, C. F., Cao, Z. N., and Luo, W. (2007). "Acetylation of wheat straw hemicelluloses in ionic liquid using iodine as a catalyst," *Carbohydrate Polymers* 70(4), 406-414. DOI: 10.1016/j.carbpol.2007.04.022

Swatloski, R. P., Spear, S. K., Holbrey, J. D., and Rogers, R. D. (2002). "Dissolution of cellose with ionic liquids," *Journal of the American Chemical Society* 124(18), 4974-4975. DOI: 10.1021/ja025790m

Zhang, T., Liu, X., Jiang, M., Duan, Y., and Zhang, J. (2015). "Effect of cellulose solubility on the thermal and mechanical properties of regenerated cellulose/graphene nanocomposites based on ionic liquid 1-allyl-3-methylimidazoliun chloride," *RSC Adv*. 5(93), 76302-76308. DOI: 10.1039/C5RA15160K

Zhang, Y. Hs., Berson, E., Sarkanen, S., and Dale, B. E. (2009). "Sessions 3 and 8: Pretreatment and biomass recalcitrance: Fundamentals and progress," *Applied Biochemistry and Biotechnology* 153(1-3), 80-83. DOI: 10.1007/s12010-009-8610-3

Zhang, Y. H. P. (2008). "Reviving the carbohydrate economy *via* multi-product lignocellulose biorefineries," *Journal of Industrial Microbiology & Biotechnology* 35(5), 367-375. DOI: 10.1007/s10295-007-0293-6

Article submitted: May 4, 2016; Peer review completed: July 17, 2016; Revised version received and accepted: July 26, 2016; Published: September 28, 2016.
DOI: 10.15376/biores.11.4.9710-9722